Proceedings of the ASME 2018 International Design Engineering Technical Conferences & Computers and Information in Engineering Conference
IDETC/CIE 2018
August 26-29, 2018, Quebec City, Canada

DETC2018-85998

STATIC AND STABILITY ANALYSIS OF A PLANAR COMPLIANT TENSEGRITY MECHANISM

Miranda M. Tanouye **Vishesh Vikas**
Agile Robotics Laboratory
Department of Mechanical Engineering
University of Alabama
Tuscaloosa, Alabama 35487
Email: mmtanouye@crimson.ua.edu, vvikas@eng.ua.edu

ABSTRACT

Traditional tensegrity mechanisms are comprised of compressive (rigid rods) and tensile members (strings). Compliant tensegrity mechanisms (CoTM) introduce springs alongside strings and rods, allowing these structures to be more adaptable and robust. The kinematic and stability analyses of such mechanisms will facilitate better behavioral understanding for control of such structures. Generally, the kinematic analysis assumes zero-free length (ZFL) springs which facilitates simplification of equations of motion. However, a general ZFL does not exist and the relaxation of ZFL assumption for a CoTM introduces computational complexities resulting from their non-linear nature. The research considers equilibrium and stability analysis of a planar CoTM mechanism consisting of two triangular platforms connected by a compressive member and two spring elements. For an assumed numerical example, the analysis illustrates the increase in computation complexity, and non-linear behavior of equilibrium and stable solutions as assumption is relaxed from 1) both spring ZFL, to 2) one spring ZFL, and 3) no spring ZFL.

NOMENCLATURE

${}^{A}\boldsymbol{P}_i$ Point i represented in coordinate system A
$\boldsymbol{P}_{i\to j}$ Vector between points i and j

INTRODUCTION

Tensegrity mechanisms are made up of compressive and tensile members where no pair of struts touch and each end is connected to three non-coplanar ties. This provides some unique features: strain is distributed through deformation of the structure, they expand in all axes at once, and can be built from one another [1]. These unique properties are make them useful in the fields of robotics [2, 3], space applications [4], bridges [5] and biological modeling [6]. Several natural structures can be modeled as a tensegrity, such as the human spine [7] and DNA molecules [8]. Their ability to withstand large amounts of strain and efficient packing (occupying less volume for storage) make them ideal for deployment applications [9].

Static analysis, dynamic and stability analysis of traditional tensegrity mechanism provide insight into their behavior [10–14]. The direct static problem yields equilibrium equations which are are non-linear in the angle, thus, yielding multiple equilibrium solutions. The analytical solution structure of the equilibrium equations are of special interest as they are helpful in providing the bound on the number of possible solutions. Some analytical solutions for prestressed tensegrity stuctures have been proposed and explored [15–17].

Compliant Tensegrity Mechanisms (CoTM) augment traditional tensegrity structures by adding springs elements that can compress and also extend. Moreover, the mechanism orientation may be controlled through its compliance, such as, by indirectly varying free lengths of the spring elements. Such modifications

have been experimentally introduced to build tensegrity robots, however, their kinematic analysis has been limited [17–20]. The presented research analyzes the effect of variation of spring free lengths on the static equilibrium and stability of a planar tensegrity mechanism.

Commonly, the static and dynamic analysis of these structures assumes zero free lengths (ZFL). For a ZFL spring, the unstretched (free) length of a linear spring is zero and a general ZFL spring is not an existing product [21]. This greatly simplifies the analysis of the system, however this assumption is not valid for actual systems. The paper presents detailed analysis for an example planar CoTM where ZFL assumption is gradually relaxed 1) both springs have ZFL, 2) one spring has ZFL and 3) no springs have ZFLs.

PROBLEM STATEMENT

The proposed mechanism consists of two triangular rigid bodies connected by a rigid rod and two springs members as shown in Fig. 1 where the relative distance between points $1,4$ is L_3. The spring free lengths and spring constants are denoted by L_{0i}, k_i where $i = 1,2$.

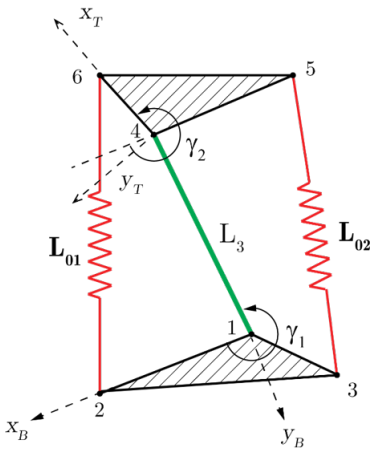

FIGURE 1. THE PROPOSED PLANAR COMPLIANT TENSEGRITY MECHANISM (COTM) COMPRISES OF TWO TRIANGULAR RIGID BODIES CONNECTED BY A RIGID ROD (GREEN) AND TWO SPRING MEMBERS (RED)

The objective is to find all of its stable equilibrium positions, as defined by γ_1 and γ_2, for a given set of parameters.

PROBLEM DEFINITION

Let the coordinate system B be fixed on the bottom rigid body with origin at point 1, x-axis between points 1, 2 and z-axis out of the plane of paper. Similarly, the coordinate system T is fixed on the top rigid body with origin at point 4, x-axis between points 4, 6 and z-axis out of the plane of paper. The points are

$$ {}^B\boldsymbol{P}_2 = [p_{2x}, 0, 0]^T \ , \quad {}^B\boldsymbol{P}_3 = [p_{3x}, p_{3y}, 0]^T \tag{1} $$

$$ {}^T\boldsymbol{P}_5 = [p_{5x}, 0, 0]^T \ , \quad {}^T\boldsymbol{P}_6 = \left[p_{6x}, p_{6y}, 0\right]^T \tag{2} $$

The transformation matrix ${}^T_B\boldsymbol{T}$ between coordinate system T and B is written as

$$ {}^T_B\boldsymbol{T} = \begin{bmatrix} c_2 & -s_2 & 0 & L_3 c_1 \\ s_2 & c_2 & 0 & L_3 s_1 \\ 0 & 0 & 1 & 0 \\ 0 & 0 & 0 & 1 \end{bmatrix} \tag{3} $$

where c_i, s_i are $\cos\gamma_i, \sin\gamma_i$ corresponding to angles γ_1, γ_2 shown in Fig. 1. Hence, for $i = 4,5$

$$ \begin{bmatrix} {}^B\boldsymbol{P}_i \\ 1 \end{bmatrix} = {}^T_B\boldsymbol{T} \begin{bmatrix} {}^T\boldsymbol{P}_i \\ 1 \end{bmatrix} \tag{4} $$

The superscript will be dropped for remaining section of the paper as all the calculations will be performed in the B coordinate system.

The static equilibrium equations for force and torque balance yield

$$ \begin{aligned} \boldsymbol{F} &= f_1 \left(\frac{\boldsymbol{P}_{2\to6}}{d_1} \right) + f_2 \left(\frac{\boldsymbol{P}_{3\to5}}{d_2} \right) + f_3 \left(\frac{\boldsymbol{P}_{1\to4}}{L_3} \right) && = 0 \\ F &= \frac{f_1}{d_1} \left(\boldsymbol{P}_{1\to4} \times \boldsymbol{P}_{2\to6} \right) + \frac{f_2}{d_2} \left(\boldsymbol{P}_{1\to4} \times \boldsymbol{P}_{3\to5} \right) && = 0 \quad (5) \\ \tau &= \boldsymbol{P}_{1\to2} \times \left(f_1 \cdot \frac{\boldsymbol{P}_{2\to6}}{d_1} \right) + \boldsymbol{P}_{1\to3} \times \left(f_2 \cdot \frac{\boldsymbol{P}_{3\to5}}{d_2} \right) && = 0 \quad (6) \end{aligned} $$

where f_3 is the unknown force along the rigid bar, $f_i = k_i(d_i - L_{0i})$ are the forces in spring elements and d_i are length of the spring elements $\forall i = 1,2$. The four equations of interest are two equilibrium equations

$$ k_1 \left(1 - \frac{L_{01}}{d_1} \right) \left(\boldsymbol{P}_{1\to4} \times \boldsymbol{P}_{2\to6} \right) + k_2 \left(1 - \frac{L_{02}}{d_2} \right) \left(\boldsymbol{P}_{1\to4} \times \boldsymbol{P}_{3\to5} \right) = 0 \tag{7} $$

$$ k_1 \left(1 - \frac{L_{01}}{d_1} \right) \left(\boldsymbol{P}_{1\to2} \times \boldsymbol{P}_{2\to6} \right) + k_2 \left(1 - \frac{L_{02}}{d_2} \right) \left(\boldsymbol{P}_{1\to3} \times \boldsymbol{P}_{3\to5} \right) = 0 \tag{8} $$

coupled with two constraint equations

$$ d_1^2 - \| \boldsymbol{P}_{2\to6} \|^2 = 0 \tag{9} $$

$$ d_2^2 - \| \boldsymbol{P}_{3\to5} \|^2 = 0 \tag{10} $$

CASE 1: BOTH SPRINGS HAVE ZFL

Equilibrium Analysis

For this first case, both springs are assumed to have ZFL i.e. $L_{01} = L_{02} = 0$. Hence, Eqns. (5) and (6) simplify to the following

$$\begin{aligned} F &= k_2(-c_1 L_3 p_{3y} - c_2 p_{3y} p_{5x} + c_2 p_{3x} p_{5y} + L_3 p_{3x} s_1 + \\ &\quad p_{3x} p_{5x} s_2 + p_{3y} p_{5y} s_2) + k_1 p_{2x}(L_3 s_1 + p_{6x} s_2) \quad (11) \\ \tau &= L_3[k_1 s_1(p_{2x} - c_2 p_{6x}) + c_1 k_1 p_{6x} s_2 + c_1 k_2(-p_{3y} + \\ &\quad c_2 p_{5y} + p_{5x} s_2) + k_2 s_1(p_{3x} - c_2 p_{5x} + p_{5y} s_2)] \quad (12) \end{aligned}$$

Importantly, the variables d_1 and d_2 do not appear in the equilibrium equations as a result of ZFL assumption. These equations can be converted to polynomial equations using the tan-half angle identities where

$$c_i = \frac{1 - x_i^2}{1 + x_i^2}\ ,\ s_i = \frac{2x_i}{1 + x_i^2} \quad \text{where} \quad x_i = \tan\frac{\gamma_i}{2} \quad i = 1, 2 \quad (13)$$

Substituting Eqn. (13) into Eqns. (11) and (12) and rearranging produces

$$\begin{aligned} F &= (A_1 x_2^2 + A_2 x_2 + A_3) x_1^2 + (A_4 x_2^2 + A_5 x_2 + A_6) x_1 + \\ &\quad (A_7 x_2^2 + A_8 x_2 + A_9) \quad (14) \\ \tau &= (B_1 x_2^2 + B_2 x_2 + B_3) x_1^2 + (B_4 x_2^2 + B_5 x_2 + B_6) x_1 + \\ &\quad (B_7 x_2^2 + B_8 x_2 + B_9) \quad (15) \end{aligned}$$

Where the A_i and B_i coefficients are listed in Appendix A. Eqns. (14) and (15) may be rewritten by combing their A_i and B_i coefficients

$$\begin{aligned} F &= C_1 x_1^2 + C_2 x_1 + C_3 \quad (16) \\ \tau &= D_1 x_1^2 + D_2 x_1 + D_3 \quad (17) \end{aligned}$$

The solution of this system of equations can be obtained by constructing a Sylvester matrix [22] from the combined coefficients for x_1 in Eqns. (16) and (17) to create a linear system of the form

$$\begin{bmatrix} C_1 & C_2 & C_3 & 0 \\ 0 & C_1 & C_2 & C_3 \\ D_1 & D_2 & D_3 & 0 \\ 0 & D_1 & D_2 & D_3 \end{bmatrix} \begin{bmatrix} x_1^3 \\ x_1^2 \\ x_1 \\ 1 \end{bmatrix} = \begin{bmatrix} 0 \\ 0 \\ 0 \\ 0 \end{bmatrix} \quad (18)$$

As these system of equations has a non-trivial solution, the determinant of the Sylvester matrix needs to be zero. This determinant will result in a sixth (6) degree polynomial in variable x_2 and can be used to solve for the solutions of x_2. Importantly, there is a one-to-one mapping between x_1 and x_2 i.e. for a given solution of x_2, there exists a unique x_1. The unique x_1 can be calculated by rearranging Eqn. (18) and substituting x_2 into the coefficients. Thereafter, unique values for γ_1 and γ_2 can be calculated for each x_1 and x_2 value from Eqn. (13).

$$\begin{bmatrix} x_1^3 \\ x_1^2 \\ x_1 \end{bmatrix} = \begin{bmatrix} C_1 & C_2 & C_3 \\ 0 & C_1 & C_2 \\ D_1 & D_2 & D_3 \end{bmatrix}^{-1} \begin{bmatrix} 0 \\ -C_3 \\ 0 \end{bmatrix} \quad (19)$$

Stability Analysis

The interest of this study is not only evaluating all possible solutions of a given system, but determining the stability of these solutions. This is done by evaluating constructing the Jacobian and observing its eigenvalues. The Jacobian was constructed from the force and torque equations with respect to the dependent variables x_1 and x_2

$$\boldsymbol{J}_{case1} = \begin{bmatrix} F_{x_1} & F_{x_2} \\ \tau_{x_1} & \tau_{x_2} \end{bmatrix} \quad (20)$$

where $A_x = \dfrac{\partial A}{\partial x}$. From there, the eigenvalues of J can then be evaluated with the found x_1, x_2 solutions. The corresponding solution is stable if real parts of all the eigenvalues are negative.

CASE 2: ONE ZERO FREE LENGTH

Equilibrium Analysis

For this case, only the second spring is assumed to have ZFL i.e. $L_{01} \neq 0, L_{02} = 0$. This introduces a third variable, d_1, into the equilibrium equations and couples them with the constraint Eqn. (9) corresponding to d_1. After using the tan-half angle trigonometric identity for polynomial conversion, two equilibrium and the coupled constraint equation can be written as

$$\begin{aligned} F &= (E_{11} d_1 + E_{12}) x_1^2 + (E_{21} d_1 + E22) x_1 + (E_{31} d_1 + E_{32}) \quad (21) \\ \tau &= (F_{11} d_1 + F_{12}) x_1^2 + (F_{21} d_1 + F22) x_1 + (F_{31} d_1 + F_{32}) \quad (22) \\ C_1 &= (1 + x_1^2)(1 + x_2^2) d_1^2 - (G_1 x_1^2 + G_2 x_1 + G_3) \quad (23) \end{aligned}$$

where E_i, F_i and G_i coefficients are polynomials only dependent on x_2, and are defined in Appendix B. To reduce the system to two polynomials (x_1, x_2), d_1 is solved for from the force and torque equations (d_{1F} and $d_{1\tau}$) and substituted into Eqn. 23.

$$d_{1F} = \frac{H_1}{H_2}\ ,\ d_{1\tau} = \frac{I_1}{I_2} \quad (24)$$

where H_i and I_i coefficients are listed in Appendix C. The mentioned substitution of d_{1F} and $d_{1\tau}$ results in two new polynomials (C_{1F} and $C_{1\tau}$) only dependent on x_1 and x_2.

$$C_{1F} = J_1x_1^6 + J_2x_1^5 + J_3x_1^4 + J_4x_1^3 + J_5x_1^2 + J_6x_1 + J_7 \quad (25)$$
$$C_{1\tau} = K_1x_1^6 + K_2x_1^5 + K_3x_1^4 + K_4x_1^3 + K_5x_1^2 + K_6x_1 + K_7 \quad (26)$$

J_i and K_i are polynomials of x_2 to the 6th degree and are used to form a Sylvester matrix dependent only on x_2, similar to how Eqn. (18) was constructed for the previous case. Since C_{1F} and $C_{1\tau}$ are polynomials to the 6th degree, the Sylvester matrix is a 12×12 matrix with a corresponding 12×1 vector which spans from x_1^{11} to 1. The resulting Sylvester matrix is singular and the determinant results in a 72 degree polynomial in variable x_2. Once the determinant is found, solving for x_2 and x_1 is the same as for case 1, except x_1 values are the 11th element of the vector, not the 3rd. Substituting the corresponding x_1 and x_2 values into either d_{1F} or $d_{1\tau}$ from Eqn. (24) calculates the corresponding d_1 value.

Stability Analysis

The Jacobian was constructed from Eqns. (21), (22) and (23) with respect to three variables x_1, x_2 and d_1

$$\boldsymbol{J}_{case2} = \begin{bmatrix} F_{x_1} & F_{x_2} & F_{d_1} \\ \tau_{x_1} & \tau_{x_2} & \tau_{d_1} \\ C_{1,x_1} & C_{1,x_2} & C_{1,d_1} \end{bmatrix} \quad (27)$$

Determining stability is then accomplished as described in case 1, where a solution is considered stable when all real parts of the corresponding eigenvalues of the Jacobian are negative.

CASE 3: BOTH NON ZERO FREE LENGTH

For the final case, ZFL constraint for both the springs are relaxed. As a result, the complexity increases as another variable d_2 is introduced into the system of equations from the constraint equation Eqn. (10). The resulting constraint equations C_2 is the same as how C_1 was developed for d_1 in case 2. Now the system is defined by the following force, torque, and constraint equations. L_i, M_i, N_i and O_i coefficients are listed in Appendix D.

$$F = L_1x_1^2 + L_2x_1 + L_3 \quad (28)$$
$$\tau = M_1x_1^2 + M_2x_1 + M_3 \quad (29)$$
$$C_1 = (1+x_1^2)(1+x_2^2)d_1^2 - (N_1x_1^2 + N_2x_1 + N_3) \quad (30)$$
$$C_2 = (1+x_1^2)(1+x_2^2)d_2^2 - (O_1x_1^2 + O_2x_1 + O_3) \quad (31)$$

TABLE 1. CASE 1 CoTM PARAMETERS

Parameter	Value
L_3	9 m
k_1, k_2	2.81 $\frac{N}{m}$
p_{2x}	3.1875 m
p_{3x}, p_{3y}	-2.5745, 4.9309 m
p_{6x}	4.25 m
p_{5x}, p_{5y}	-0.299, -3.4872 m

TABLE 2. CASE 1 SOLUTIONS

Solution	γ_1, deg	γ_2, deg
1	75.034	289.0393
2	276.53	330.7859
3	252.35	123.7358
4	93.673	124.9667
5	-149.7952-85.4127i	-160.7121-167.3794i
6	-149.7952+85.4127i	-160.7121+167.3794i

Stability Analysis

Again, the Jacobian was constructed in the same manner as Case 1 and 2 from Eqns. (28)-(31).

$$\boldsymbol{J}_{case3} = \begin{bmatrix} F_{x_1} & F_{x_2} & F_{d_1} & F_{d_2} \\ \tau_{x_1} & \tau_{x_2} & \tau_{d_1} & \tau_{d_2} \\ C_{1,x_1} & C_{1,x_2} & C_{1,d_1} & C_{1,d_2} \\ C_{2,x_1} & C_{2,x_2} & C_{2,d_1} & C_{2,d_2} \end{bmatrix} \quad (32)$$

Stability is then determined observing the real part of the eigenvalues of $\boldsymbol{J}_{case3}$ from Eqn. (32).

NUMERICAL EXAMPLES AND DISCUSSION

Case 1: Six solutions were determined based on the given parameters in Tab. 1 and are listed in Tab. 2. Of these, only solution 3 was found to be stable. The four real solutions are illustrated in Fig. 2, with the stable solution in bold.

Case 2: A total of 72 possible solutions were found for the given parameters described in Tab. 1 where $L_{01} = 11.5$ m. Of those, 14

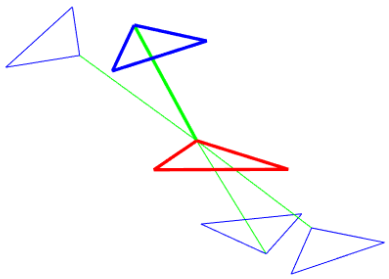

FIGURE 2. VISUALIZATION OF SOLUTIONS FOR CASE 1: THE FIGURE SHOWS FOUR REAL SOLUTIONS WHERE THE BOTTOM RIGID BODY (RED) IS FIXED. THE TOP RIGID BODY AND COMPRESSIVE RIGID MEMBER ARE MAKED IN BLUE AND GREEN RESPECTIVELY. THE ONE STABLE SOLUTION IS MARKED IN BOLD.

were real and are listed in Tab. 3. Solutions 8, 12 and 14 were determined stable and are shown as bold in Fig. 3.

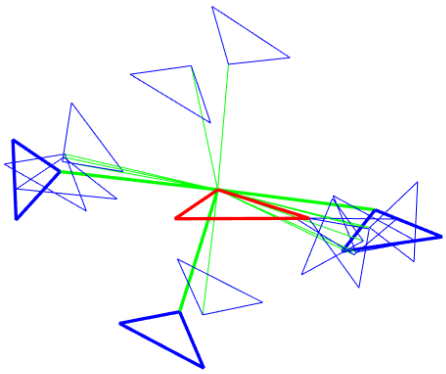

FIGURE 3. VISUALIZATION OF SOLUTIONS FOR CASE 2: THE ZFL ASSUMPTION IS RELAXED FOR ONE SPRING ELEMENT. FOURTEEN (14) REAL SOLUTIONS ARE SHOWN WITH THE THREE (3) STABLE SOLUTIONS MARKED IN BOLD.

TABLE 3. CASE 2 SOLUTIONS FOR L_{01}=11.5 m

Solution	γ_1, deg	γ_2, deg	d_1, m
1	121.6928	-170.2946	13.9540
2	-53.7043	-137.7794	10.1598
3	-134.6342	-118.0702	-15.3495
4	109.4200	-113.0299	9.0803
5	43.8350	-111.0978	-2.8799
6	108.0598	-79.0483	6.7786
7	115.1896	-5.9702	-8.1922
8	-49.0604	13.5862	-8.9689
9	121.0391	41.4523	11.5033
10	-121.2006	64.2291	-7.1420
11	-57.2079	65.8622	5.0324
12	35.4058	67.8622	-10.8074
13	-55.7211	94.4550	-3.5558
14	129.9898	112.1813	-15.1380

Case 3: Using the Bertini software [23], 88 solutions were found for Case 3 using the parameters listed in Tab. 1, and $L_{01} = L_{02} = 11.5$ m. Of those solutions, 30 were real and solutions 14, 15, 26, 28 and 29 were determined stable. Figure 4 showcases all real solutions with the stable solutions in bold.

Discussion

A diagram of γ_1 and γ_2 solutions were plotted against varying L_{01} values, as seen in Figs. 5 and 6. It is interesting to see that the 4 real solutions found in case 1 for ZFL branch off for both γ_1 and γ_2. This implies that it is possible to move from one orientation to another by slowly shortening or lengthening the free length of L_{01} and thus controlling the mechanisms movement. This can be done by altering the length of the string on the string-spring series combination of the tensile element of the mechanism. It also shows that as free length increases, the behavior of the system changes and the number of stable equilibrium solutions vary.

Results for γ_1 and γ_2 also show a slight inverse of themselves. The top set and bottom set of solutions for each are very similar in terms of pattern, especially for γ_1. This may imply that for some solutions there is a mirrored configuration and solution.

Stable solutions are marked on Figs. 5 and 6 with crosses. For γ_1 they start to appear when L_{01}=0.4 m and tend to follow

TABLE 4. CASE 3 SOLUTIONS FOR $L_{01} = L_{02} = 11.5$ m

Solution	γ_1, deg	γ_2, deg	d_1, m	d_2, m
1	118.7485	35.5190	11.1259	0.0557
2	1.8614	11.3066	-10.0386	14.4543
3	123.6903	48.3537	-11.9335	0.0016
4	158.8463	147.9065	-16.1491	3.8760
5	27.0083	-135.4189	2.1149	8.5604
6	81.5837	-60.6132	-5.2044	-2.6186
7	114.3792	24.2121	10.3910	-0.0340
8	113.3238	148.8744	-14.7436	-6.2564
9	158.4532	-18.3662	-7.7777	8.6587
10	121.9622	43.8495	-11.6539	-0.0012
11	-16.1066	152.1678	1.7764	13.8590
12	1.5492	-177.3439	-1.5645	11.7686
13	116.1954	-141.8103	11.8299	6.9187
14	-99.1546	157.6979	11.2257	11.0492
15	-178.9477	-69.8945	11.5000	11.5000
16	-109.3430	109.1438	-8.7881	-12.9117
17	-60.0250	49.9528	6.0817	-17.9499
18	-119.6207	-94.0043	14.4379	13.3260
19	-82.2511	-172.0681	11.3387	10.9626
20	-92.6299	-46.7762	-12.1071	-16.1023
21	-173.9013	5.3089	7.9248	11.3328
22	-1.0256	-33.8180	9.6776	12.2169
23	-59.0255	-143.6933	10.4229	-11.0586
24	111.373	16.3881	-9.8738	-0.0018
25	52.6240	85.5612	11.6834	11.6098
26	56.0999	108.9002	11.5000	11.5000
27	118.6869	-152.4669	12.7409	-6.9239
28	48.0180	60.9639	11.5000	11.5000
29	-60.2020	-120.6541	11.5000	11.5000
30	113.2537	21.2901	-10.1985	0.0013

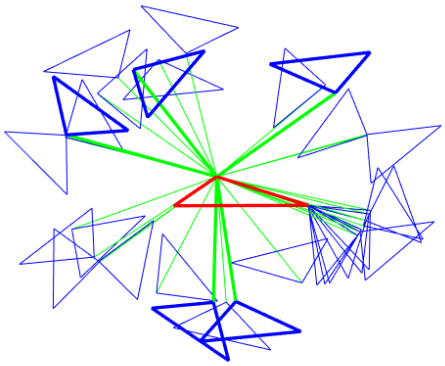

FIGURE 4. VISUALIZATION OF SOLUTIONS FOR CASE 3: THE ZFL ASSUMPTION IS RELAXED FOR BOTH SPRINGS AND THIRTY (30) REAL SOLUTIONS RESULT FROM NUMERICALLY SOLVING THE EXAMPLE VALUES. THE FIVE (5) STABLE SOLUTIONS ARE MARKED IN BOLD.

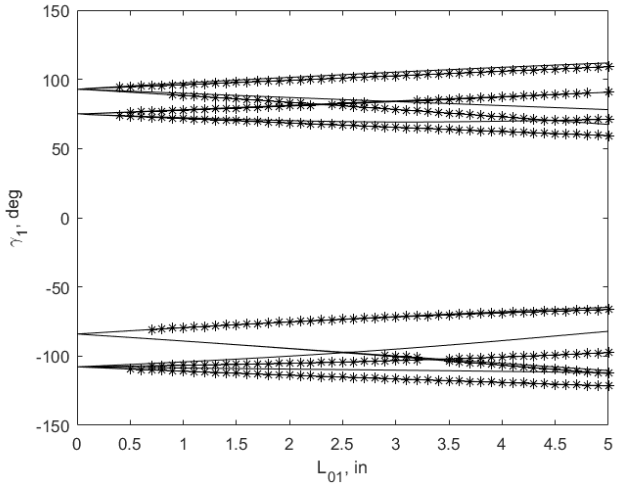

FIGURE 5. γ_1 SOLUTIONS FOR VARYING L_{01} WITH MARKED STABLE SOLUTIONS.

one bifurcation line. Where these lines intersect, the system loses stability except for around (4.5 m, 77.35 deg) where the stable solutions start to follow the line they intersected with.

Figure 6 doesn't show the same interrupt for stable solutions of γ_2 where the bifurcation lines intersect as they do for γ_1. No stable solutions were determined at L_{01}=0 m, however solution 3 in Tab. 2 for case 1 was determined stable. This is expected

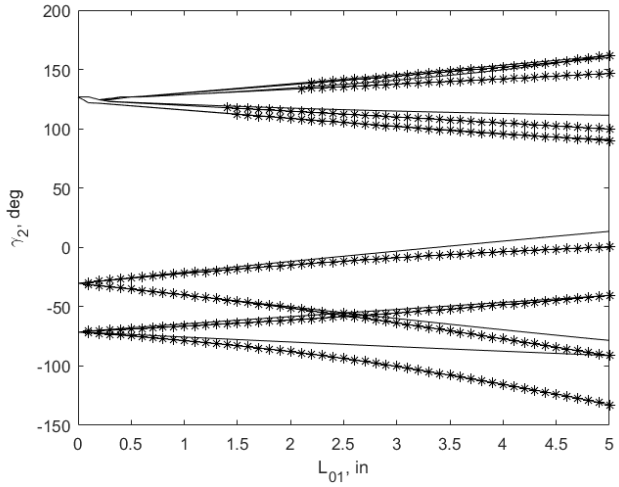

FIGURE 6. γ_2 SOLUTIONS FOR VARYING L_{01} WITH MARKED STABLE SOLUTIONS.

because when adding the third equation for C_1 into the system it made the Sylvester matrix in Eqn. (18) redundant, thus no stable solutions. However, the gap between 0 and 0.5 m for γ_1 and 0 and 1.5 m for γ_2 is unexpected and interesting to note. Lack of stable solutions may be due to a computational error or a higher degree for the derivative of the Jacobian needs to be calculated.

A Sylvester matrix could not be used for Case 3 as it was for Case 1 and 2 due to the complexity of the polynomials. The Bertini software was used instead to solve for the solutions, as a result, the degree of the polynomial remains unknown and correspondingly, the total number of possible solutions.

From Case 1 to Case 3, the overall complexity of this simple planar example has increased greatly. Moving forward to a 3D example is only expected to increase in complexity further. Finding better methods for solving these complex polynomials will be a continuous problem in this study.

CONCLUSION

This paper presented a method for determining the stable equilibrium solutions for a planar compliant tensegrity mechanism that is comprised of two rigid bodies connected by a compressive member and two spring members. Complexity of the problem increased dramatically from assuming a) both ZFL springs - sixth degree polynomial corresponding to equilibrium orientations; b) only one spring ZFL - 72 degree polynomial; c) no ZFL spring - 88 numerical solutions for example problem but unknown degree of polynomial using homotopy-based Bertini numerical software. The resulting behavior of the mechanism as ZFL assumption for one spring is relaxed and varied is also observed. Here, the stable solutions show how to control the configuration of the mechanism through compliance of the springs by shortening or lengthening its free length. This control is possible by varying L_{01} to move between desired γ_1 solutions.

REFERENCES

[1] Pugh, A., 1976. *An Introduction to Tensegrity*. The Dome series. University of California Press.

[2] Shibata, M., Saijyo, F., and Hirai, S., 2009. "Crawling by body deformation of tensegrity structure robots". In 2009 IEEE International Conference on Robotics and Automation, pp. 4375–4380.

[3] Iscen, A., Agogino, A., SunSpiral, V., and Tumer, K., 2014. "Flop and roll: learning robust goal-directed locomotion for a tensegrity robot". In IEEE/RSJ International Conference on Intelligent Robots and Systems, pp. 2236–2243.

[4] Tibert, G., 2002. "Deployable tensegrity structures for space applications". PhD Thesis, KTH Royal Institute of Technology, Sweden.

[5] Veuve, N., Dalil Safaei, S., and Smith, I. F. C., 2016. "Active control for mid-span connection of a deployable tensegrity footbridge". *Engineering Structures,* ***112***, Apr., pp. 245–255.

[6] Ingber, D. E., 1998. "The architecture of life". *Scientific American,* ***278***(1), pp. 48–57.

[7] Levin, S. M., 2002. "The tensegrity-truss as a model for spine mechanics: biotensegrity". *Journal of mechanics in medicine and biology,* ***2***(03n04), pp. 375–388.

[8] Liedl, T., Hgberg, B., Tytell, J., Ingber, D. E., and Shih, W. M., 2010. "Self-assembly of three-dimensional prestressed tensegrity structures from DNA". *Nature Nanotechnology,* ***5***(7), July, pp. 520–524.

[9] Cornel Sultan, and Robert T. Skelton, 1998. "Tendon control deployment of tensegrity structures". In Smart Structures and Materials 1998: Mathematics and Control in Smart Structures, Vol. 3323, pp. 3323–12.

[10] Juan, S. H., and Mirats Tur, J. M., 2008. "Tensegrity frameworks: Static analysis review". *Mechanism and Machine Theory,* ***43***(7), July, pp. 859–881.

[11] Zhang, J., and Ohsaki, M., 2007. "Stability conditions for tensegrity structures". *International Journal of Solids and Structures,* ***44***(11), June, pp. 3875–3886.

[12] Murakami, H., 2001. "Static and dynamic analyses of tensegrity structures. Part II. Quasi-static analysis". *International Journal of Solids and Structures,* ***38***(20), May, pp. 3615–3629.

[13] Connelly, R., and Whiteley, W., 1996. "Second-Order Rigidity and Prestress Stability for Tensegrity Frameworks". *SIAM Journal on Discrete Mathematics,* ***9***(3), Aug., pp. 453–491.

[14] Arsenault, M., and Gosselin, C. M., 2006. "Kinematic, static and dynamic analysis of a planar 2-dof tensegrity

mechanism". *Mechanism and Machine Theory,* ***41***(9), Sept., pp. 1072–1089.

[15] Sultan, C., Corless, M., and Skelton, R. E., 2001. "The prestressability problem of tensegrity structures: some analytical solutions". *International Journal of Solids and Structures,* ***38***(30), July, pp. 5223–5252.

[16] Pellegrino, S., 1990. "Analysis of prestressed mechanisms". *International Journal of Solids and Structures,* ***26***(12), Jan., pp. 1329–1350.

[17] Crane, C. D., Bayat, J., Vikas, V., and Roberts, R., 2008. "Kinematic Analysis of a Planar Tensegrity Mechanism with Pre-Stressed Springs". In *Advances in Robot Kinematics: Analysis and Design*, J. Lenari and P. Wenger, eds. Springer Netherlands, Dordrecht, pp. 419–427.

[18] Vasquez, R. E., and Correa, J. C., 2007. "Kinematics, dynamics and control of a planar 3-dof tensegrity robot manipulator". In ASME International Design Engineering Technical Conferences and Computers and Information in Engineering Conference, pp. 855–866.

[19] Vasquez, R. E., Crane, III, C. D., and Correa, J. C., 2014. "Analysis of a planar tensegrity mechanism for ocean wave energy harvesting". *Journal of Mechanisms and Robotics,* ***6***(3), June, pp. 031015–031015–12.

[20] Vikas, V., 2008. "Kinematic analysis of a planar tensegrity mechanism with pre-stressed springs". Master's thesis, University of Florida, United States.

[21] Delissen, A. A. T. M., Radaelli, G., and Herder, J. L., 2017. "Design and optimization of a general planar zero free length spring". *Mechanism and Machine Theory,* ***117***, Nov., pp. 56–77.

[22] Sylvester, J. J., 1853. "On a theory of the syzygetic relations of two rational integral functions, comprising an application to the theory of sturm's functions, and that of the greatest algebraical common measure". *Philosophical Transactions of the Royal Society of London,* ***143***, pp. 407–548.

[23] Bates, D. J., Hauenstein, J. D., Sommese, A. J., and Wampler, C. W. Bertini: Software for numerical algebraic geometry. Available at bertini.nd.edu.

Appendix A: Coefficients for Eqns. (14), (15)

$$
\begin{aligned}
A_1 &= L_3(k_2p_{3y}+k_2p_{5y})\\
A_2 &= -L_3(2k_1p_{6x}+2k_2p_{5x})\\
A_3 &= L_3(k_2p_{3y}-k_2p_{5y})\\
A_4 &= L_3(2k_1p_{2x}+2k_2p_{3x}+2k_1p_{6x}+2k_2p_{5x})\\
A_5 &= 4L_3k_2p_{5y}\\
A_6 &= L_3(2k_1p_{2x}+2k_2p_{3x}-2k_1p_{6x}-2k_2p_{5x})\\
A_7 &= -L_3(k_2p_{3y}+k_2p_{5y})\\
A_8 &= L_3(2k_1p_{6x}+2k_2p_{5x})\\
A_9 &= -L_3(k_2p_{3y}-k_2p_{5y})\\
B_1 &= L_3k_2p_{3y}-k_2p_{3x}p_{5y}+k_2p_{5x}p_{3y}\\
B_2 &= 2k_1p_{2x}p_{6x}+2k_2p_{3x}p_{5x}+2k_2p_{3y}p_{5y}\\
B_3 &= L_3k_2p_{3y}+k_2p_{3x}p_{5y}-k_2p_{5x}p_{3y}\\
B_4 &= 2L_3k_1p_{2x}+2L_3k_2p_{3x}\\
B_5 &= 0\\
B_6 &= 2L_3k_1p_{2x}+2L_3k_2p_{3x}\\
B_7 &= k_2p_{5x}p_{3y}-k_2p_{3x}p_{5y}-L_3k_2p_{3y}\\
B_8 &= 2k_1p_{2x}p_{6x}+2k_2p_{3x}p_{5x}+2k_2p_{3y}p_{5y}\\
B_9 &= k_2p_{3x}p_{5y}-l_3k_2p_{3y}-k_2p_{5x}p_{3y}
\end{aligned}
$$

Appendix B: Coefficients for Eqns. (21)-(23)

$$
\begin{aligned}
E_1 =&(L_3(d_1k_2p_{3y}+d_1k_2p_{5y}))x_2^2\\
&+(-L_3(2d_1k_1p_{6x}-2L_{01}k_1p_{6x}+2d_1k_2p_{5x}))x_2\\
&+L_3(d_1k_2p_{3y}-d_1k_2p_{5y})\\
E_2 =&(L_3(2d_1k_1p_{2x}-2L_{01}k_1p_{6x}-2L_{01}k_1p_{2x}+2d_1k_2p_{3x}\\
&+2d_1k_1p_{6x}+2d_1k_2p_{5x}))x_2^2+(4L_3d_1k_2p_{5y})x_2\\
&-L_3(2L_{01}k_1p_{2x}-2L_{01}k_1p_{6x}-2d_1k_1p_{2x}-2d_1k_2p_{3x}\\
&+2d_1k_1p_{6x}+2d_1k_2p_{5x})\\
E_3 =&(-L_3(d_1k_2p_{3y}+d_1k_2p_{5y}))x_2^2\\
&+(L_3(2d_1k_1p_{6x}-2L_{01}k_1p_{6x}+2d_1k_2p_{5x}))x_2\\
&-L_3(d_1k_2p_{3y}-d_1k_2p_{5y})\\
F_1 =&d_1k_2(L_3p_{3y}-p_{3x}p_{5y}+p_{5x}p_{3y})x_2^2\\
&+(2d_1k_1p_{2x}p_{6x}+2d_1k_2p_{3x}p_{5x}+2d_1k_2p_{3y}p_{5y}\\
&-2L_{01}k_1p_{2x}p_{6x})x_2+d_1k_2(L_3p_{3y}+p_{3x}p_{5y}-p_{5x}p_{3y})\\
F_2 =&2L_3(x_2^2+1)(d_1k_1p_{2x}-L_{01}k_1p_{2x}+d_1k_2p_{3x})\\
F_3 =&-d_1k_2(L_3p_{3y}+p_{3x}p_{5y}-p_{5x}p_{3y})x_2^2\\
&+(2d_1k_1p_{2x}p_{6x}+2d_1k_2p_{3x}p_{5x}+2d_1k_2p_{3y}p_{5y}\\
&-2L_{01}k_1p_{2x}p_{6x})x_2-d_1k_2(L_3p_{3y}-p_{3x}p_{5y}+p_{5x}p_{3y})\\
G_1 =&(L_3+p_{2x}+p_{6x})^2x_2^2+(L_3+p_{2x}-p_{6x})^2\\
G_2 =&(8L_3p_{6x})x_2\\
G_3 =&(p_{2x}-L_3+p_{6x})^2x_2^2+(L_3-p_{2x}+p_{6x})^2
\end{aligned}
$$

Appendix C: Coefficient Definitions for Eqn. (24)

$$
\begin{aligned}
H_1 =&2k_1L_{01}(p_{2x}x_1(1+x_2^2)+p_{6x}(x_2-x_1^2x_2+x_1(-1+x_2^2)))\\
H_2 =&k_2\left(p_{5y}+4p_{5y}x_1x_2-p_{5y}x_2^2+p_{5y}x_1^2(-1+x_2^2)\right.\\
&+2p_{3x}x_1(1+x_2^2)+p_{3y}(-1+x_1^2)(1+x_2^2)\\
&\left.+2p_{5x}(x_2-x_1^2x_2+x_1(-1+x_2^2))\right)+2k_1\left(p_{2x}x_1(1+x_2^2)\right.\\
&\left.+p_{6x}(x_2-x_1^2x_2+x_1(-1+x_2^2))\right)
\end{aligned}
$$

$$
\begin{aligned}
I_1 =& 2k_1L_{01}p_{2x}(p_{6x}(1+x_1^2)x_2 + L_3x_1(1+x_2^2)) \\
I_2 =& 2k_1p_{2x}(p_{6x}(1+x_1^2)x_2 + L_3x_1(1+x_2^2)) + \\
& k_2(L_3(2p_{3x}x_1 + p_{3y}(-1+x_1^2))(1+x_2^2) + \\
& (1+x_1^2)(2p_{3y}p_{5y}x_2 + p_{3y}p_{5x}(-1+x_2^2) + p_{3x}(p_{5y} + \\
& 2p_{5x}x_2 - p_{5y}x_2^2)))
\end{aligned}
$$

Appendix D: Coefficient Definitions for Eqns. (29)-(31)

$$
\begin{aligned}
L_1 =& -L_3d_1k_2(p_{3y}+p_{5y})(L_{02}-d_2)x_2^2 - L_3(2d_1d_2k_1p_{6x} + \\
& 2d_1d_2k_2p_{5x} - 2L_{01}d_2k_1p_{6x} - 2L_{02}d_1k_2p_{5x})x_2 - \\
& L_3d_1k_2(L_{02}-d_2)(p_{3y}-p_{5y}) \\
L_2 =& L_3(2d_1d_2k_1p_{2x} + 2d_1d_2k_2p_{3x} + 2d_1d_2k_1p_{6x} + 2d_1d_2k_2p_{5x} - \\
& 2L_{01}d_2k_1p_{2x} - 2L_{02}d_1k_2p_{3x} - 2L_{01}d_2k_1p_{6x} - 2L_{02}d_1k_2p_{5x})x_2^2 - \\
& 4L_3d_1k_2p_{5y}(L_{02}-d_2)x_2 + L_3(2d_1d_2k_1p_{2x} + 2d_1d_2k_2p_{3x} - \\
& 2d_1d_2k_1p_{6x} - 2d_1d_2k_2p_{5x} - 2L_{01}d_2k_1p_{2x} - 2L_{02}d_1k_2p_{3x} + \\
& 2L_{01}d_2k_1p_{6x} + 2L_{02}d_1k_2p_{5x}) \\
L_3 =& L_3d_1k_2(p_{3y}+p_{5y})(L_{02}-d_2)x_2^2 + L_3(2d_1d_2k_1p_{6x} + \\
& 2d_1d_2k_2p_{5x} - 2L_{01}d_2k_1p_{6x} - 2L_{02}d_1k_2p_{5x})x_2 + \\
& L_3d_1k_2(L_{02}-d_2)(p_{3y}-p_{5y}) \\
M_1 =& -d_1k_2(L_{02}-d_2)(L_3p_{3y} - p_{3x}p_{5y} + p_{5x}p_{3y})x_2^2 + \\
& (2d_1d_2k_1p_{2x}p_{6x} - 2L_{02}d_1k_2p_{3x}p_{5x} - 2L_{02}d_1k_2p_{3y}p_{5y} - \\
& 2L_{01}d_2k_1p_{2x}p_{6x} + 2d_1d_2k_2p_{3x}p_{5x} + 2d_1d_2k_2p_{3y}p_{5y})x_2 - \\
& d_1k_2(L_{02}-d_2)(L_3p_{3y} + p_{3x}p_{5y} - p_{5x}p_{3y}) \\
M_2 =& 2L_3(x_2^2+1)(d_1d_2k_1p_{2x} + d_1d_2k_2p_{3x} - \\
& L_{01}d_2k_1p_{2x} - L_{02}d_1k_2p_{3x}) \\
M_3 =& d_1k_2(L_{02}-d_2)(L_3p_{3y} + p_{3x}p_{5y} - p_{5x}p_{3y})x_2^2 + \\
& (2d_1d_2k_1p_{2x}p_{6x} - 2L_{02}d_1k_2p_{3x}p_{5x} - 2L_{02}d_1k_2p_{3y}p_{5y} - \\
& 2L_{01}d_2k_1p_{2x}p_{6x} + 2d_1d_2k_2p_{3x}p_{5x} + 2d_1d_2k_2p_{3y}p_{5y})x_2 + \\
& d_1k_2(L_{02}-d_2)(L_3p_{3y} - p_{3x}p_{5y} + p_{5x}p_{3y}) \\
N_1 =& G_1 \\
N_2 =& G_2 \\
N_3 =& G_3 \\
O_1 =& (L_3^2 + 2L_3p_{3x} + 2L_3p_{5x} + p_{3x}^2 + 2p_{3x}p_{5x} + p_{5x}^2 + p_{3y}^2 + \\
& 2p_{3y}p_{5y} + p_{5y}^2)x_2^2 + (4L_3p_{5y} + 4p_{3x}p_{5y} - 4p_{5x}p_{3y})x_2 + \\
& L_3^2 + 2L_3p_{3x} - 2L_3p_{5x} + p_{3x}^2 - 2p_{3x}p_{5x} + p_{5x}^2 + p_{3y}^2 - \\
& 2p_{3y}p_{5y} + p_{5y}^2 \\
O_2 =& (-4L_3p_{3y} - 4L_3p_{5y})x_2^2 + (8L_3p_{5x})x_2 + 4L_3p_{5y} - 4L_3p_{3y} \\
O_3 =& (L_3^2 - 2L_3p_{3x} - 2L_3p_{5x} + p_{3x}^2 + 2p_{3x}p_{5x} + p_{5x}^2 + p_{3y}^2 + \\
& 2p_{3y}p_{5y} + p_{5y}^2)x_2^2 + (4p_{3x}p_{5y} - 4L_3p_{5y} - 4p_{5x}p_{3y})x_2 + \\
& L_3^2 - 2L_3p_{3x} + 2L_3p_{5x} + p_{3x}^2 - 2p_{3x}p_{5x} + p_{5x}^2 + p_{3y}^2 - \\
& 2p_{3y}p_{5y} + p_{5y}^2
\end{aligned}
$$